

Textures in $^3\text{He-A}$: Hydrodynamic and magnetic effects in a slab*

Alexander L. Fetter

Institute of Theoretical Physics, Department of Physics, Stanford University, Stanford, California 94305

(Received 18 March 1976)

The Ginzburg-Landau equations are used to analyze the equilibrium configuration of $^3\text{He-A}$ in a slab, subject to either a bulk hydrodynamic flow or a uniform tipped magnetic field. Both perturbations can induce an orientational transition from an essentially uniform texture to one with large deformations. The associated phase boundaries are determined both variationally and exactly.

I. INTRODUCTION

The predicted anisotropy of superfluid $^3\text{He-A}$ has stimulated both theorists¹ and experimentalists.² The simplest example is bulk homogeneous fluid,³⁻⁶ where the orientation arises from a uniform hydrodynamic flow or a uniform static magnetic field. In a bounded domain, however, the equilibrium state generally becomes inhomogeneous, and only certain special cases have been analyzed in detail.⁷⁻¹⁰ The simplest configuration is a semi-infinite geometry, and Ambegaokar, de Gennes, and Rainer⁷ studied the static equilibrium configuration for zero flow and field with both specular and diffuse boundary conditions. de Gennes and Rainer⁸ then extended the treatment to include a uniform hydrodynamic flow in a slab, restricting themselves to the simpler case of specular boundary conditions. The rather different effect of a perpendicular magnetic field in a slab was examined by Ambegaokar and Rainer,⁹ who moreover incorporated the nuclear dipole-dipole energy. In both these latter two investigations, the superfluid state undergoes an orientational transition from a uniform state to a nonuniform one at a definite value of the flow or field that depends on the width of the channel. Such phase transitions should be detectable experimentally by NMR techniques,¹¹ and it therefore becomes interesting to undertake a more general analysis that includes both the dipole energy and an arbitrary orientation of the magnetic field. As in the more familiar case of superconductors, spatially inhomogeneous states are most tractable near the transition temperature, where a Ginzburg-Landau theory allows an essentially complete description. Section II summarizes the approximate Ginzburg-Landau free energy that serves as the basis for subsequent calculations. The orientational transitions induced by hydrodynamic flow and a static magnetic field are analyzed in Secs. III and IV, respectively, and the combined effects are considered in Sec. V.

II. GINZBURG-LANDAU FREE ENERGY

The order parameter for a spin-triplet p -wave superfluid may be expressed as a tensor $A_{\mu i}$, where the first and second indices refer to the spin and orbital vectors, respectively. (This convention follows that of Mermin and Stare,⁴ but reverses those of Leggett,¹ and of Anderson and Brinkman.¹²) In the Ginzburg-Landau regime ($T_c - T \ll T_c$), the additional part of the free-energy density that appears on entering the superfluid phase has an expansion in even powers of $A_{\mu i}$, with three distinct contributions. The bulk terms F_0 are invariant under separate rotations of the spin and orbital coordinates. This very general rotational symmetry is broken by the dipole energy F_D that couples the spin and orbital variables, leaving $F_0 + F_D$ invariant only under the simultaneous rotation of the two vectors. Even this last symmetry is broken by the various external perturbations (flow, field, walls) that orient the spin or orbital vectors. If only F_0 is considered, then the order parameter in the A phase has the special form

$$A_{\mu i} = \Delta \hat{d}_\mu (\hat{n}_1 + i\hat{n}_2)_i, \quad (1)$$

where \hat{d} , \hat{n}_1 , and \hat{n}_2 are arbitrary real unit vectors subject to the single restriction $\hat{n}_1 \cdot \hat{n}_2 = 0$. The parameters contained in F_0 fix the magnitude of Δ , and all states of the form (1) have the same free energy.

The additional contributions contain several distinct terms. First, the presence of spatial inhomogeneities leads to a kinetic energy density of the form^{1,7}

$$F_K = K_1 \partial_i A_{\mu i}^* \partial_j A_{\mu j} + K_2 \partial_i A_{\mu j}^* \partial_i A_{\mu j} + K_3 \partial_i A_{\mu j}^* \partial_j A_{\mu i}, \quad (2)$$

where repeated indices are summed from 1 to 3. Here, K_1 , K_2 , and K_3 are phenomenological constants of order $\frac{1}{5} N(0) \xi_0^2$, with $N(0) = m^* k_F / 2\pi^2 \hbar^2$,

the observed density-of-states of one spin projection at the Fermi surface, and $\xi_0 = [7\zeta(3)/48\pi^2]^{1/2} \times (\hbar v_F/k_B T_c)$. Although weak-coupling theory¹³ predicts that $K_1 = K_2 = K_3$, other cases can yield different values, and we follow Leggett¹ in retaining the more general notation. Indeed, the present analysis suggests that a direct determination of the ratio $(K_1 + K_3)/K_2$ may be feasible. Equation (2) has the immediate consequence that the fluid transports particles with current density^{7,8,14}

$$J_i = 4\hbar^{-1} \text{Im}(K_1 A_{\mu i}^* \partial_j A_{\mu j} + K_2 A_{\mu j}^* \partial_i A_{\mu j} + K_3 A_{\mu j}^* \partial_j A_{\mu i}), \quad (3)$$

and transports spin component λ with current density^{1,15}

$$J_{\lambda i}^{\sigma} = -2\epsilon_{\lambda\mu\nu} \text{Re}(K_1 A_{\mu i}^* \partial_j A_{\nu j} + K_2 A_{\mu j}^* \partial_i A_{\nu j} + K_3 A_{\mu j}^* \partial_j A_{\nu i}). \quad (4)$$

The remaining terms in the free energy are more straightforward to analyze.¹ In the presence of a magnetic field, the free-energy density acquires an additional contribution

$$F_Z = g_Z H_{\mu} A_{\mu i}^* A_{\nu i} H_{\nu}, \quad (5)$$

where g_Z is a coupling constant of order $[7\zeta(3)/24\pi^2] \chi_n (k_B T_c)^{-2} (1 + \frac{1}{4} Z_0)^{-1}$, with χ_n the normal-state static susceptibility, and $(1 + \frac{1}{4} Z_0)^{-1} \approx 4$, the Fermi-liquid enhancement factor. The walls (here taken as surfaces of constant z) may be incorporated through the boundary conditions⁷

$$A_{\mu z} = 0, \quad (6a)$$

$$\frac{\partial A_{\mu x}}{\partial z} = \frac{\partial A_{\mu y}}{\partial z} = 0, \quad (6b)$$

where only the simplest choice (specular reflection) is considered. Finally, the nuclear dipole energy couples the spin and orbital vectors, leading to a contribution

$$F_D = g_D (A_{\mu\mu}^* A_{\nu\nu} + A_{\mu\nu}^* A_{\nu\mu} - \frac{2}{3} A_{\mu\nu}^* A_{\mu\nu}), \quad (7)$$

where g_D is another coupling constant of order $(\frac{1}{10}\pi) [N(0)\gamma\hbar \ln(1.13\hbar\omega_0/k_B T_c)]^2$, with $|\gamma| \approx 2.04 \times 10^4$ (G sec)⁻¹, and $\hbar\omega_0/k_B$ a cutoff temperature of order 0.7 K. The combined volume perturbation terms are

$$F_1 = F_K + F_Z + F_D, \quad (8)$$

and the boundary conditions automatically generate the surface energy. To estimate the relative im-

portance of these various terms, note⁹ that the ratio $(g_D/g_Z)^{1/2}$ represents a characteristic magnetic field H^* of order 25 Oe, and that $(K_i/g_D)^{1/2}$ represents a characteristic length L^* of order 6×10^{-4} cm. Evidently, the magnetic field dominates the dipole energy if $H \gg H^*$, and the surface energy dominates the dipole energy for narrow channels of width $W \ll L^*$.

To make further progress, assume that the order parameter in the A phase retains its form (1) with an additional phase factor to incorporate the possibility of hydrodynamic flow. In particular, $|\Delta|$ is taken as unaffected by the presence of walls, but the direction of the unit vectors \hat{d} , \hat{n}_1 , and \hat{n}_2 can vary throughout the fluid. Although such an approximate description cannot hold arbitrarily close to T_c , it should be valid whenever the temperature-dependent coherence length $\xi_0(1 - T/T_c)^{-1/2}$ is small compared to the channel width W . This model corresponds to the London limit of Ambegaokar, de Gennes, and Rainer.⁷

Let the fluid fill the domain $|z| \leq \frac{1}{2}W$, with either a bulk flow along the \hat{y} direction or a uniform magnetic field $\vec{H} = H(\hat{y} \sin\psi + \hat{z} \cos\psi)$ in the yz plane at an angle ψ from the surface normal \hat{z} . The hydrodynamic flow may be incorporated into the order parameter with the assumed form

$$A_{\mu i}(\vec{r}) = \Delta \exp[iQy + iS(z)] [\hat{d}(z)]_{\mu} [\hat{n}_1(z) + i\hat{n}_2(z)]_i. \quad (9)$$

The first boundary condition (6a) holds if $\hat{l} \equiv \hat{n}_1 \times \hat{n}_2$ becomes normal to the wall at $z = \pm \frac{1}{2}W$, and the remaining ones (6b) require that both $d\hat{d}/dz$ and dS/dz vanish at the walls. By symmetry, \hat{l} and \hat{d} both lie in the yz plane, and we write

$$\hat{l}(z) = \hat{y} \sin\theta(z) + \hat{z} \cos\theta(z), \quad (10a)$$

$$\hat{d}(z) = \hat{y} \sin\phi(z) + \hat{z} \cos\phi(z), \quad (10b)$$

where θ and ϕ obey the boundary conditions $\theta = 0$ and $d\phi/dz = 0$ at $z = \pm \frac{1}{2}W$. These conditions differ from those of Barton and Moore,¹⁰ who mainly studied the behavior for $A_{\mu i} = 0$ at all surfaces (a model for diffuse reflection). That choice is most appropriate very near T_c , but it is incompatible with our physically motivated representation of the order parameter (9) with constant $|\Delta|$.

It is not difficult to evaluate the perturbation energy (8) for an order parameter of the form (9). Measuring lengths in units of the channel width W , we find

$$F = F_0 + F_1 = \text{const} + g_D \Delta^2 \int_{-1/2}^{1/2} [2q^2 + 2(S')^2 + 2\gamma(q \cos\theta - S' \sin\theta)^2 + (\theta')^2(1 + 2\gamma \cos^2\theta) + 2(\phi')^2(1 + \gamma \sin^2\theta)] + 2\hbar^2 \cos^2(\psi - \phi) - 2 \cos^2(\theta - \phi) \} dz, \quad (11)$$

where $q \equiv QW$, $w = W/L^*$, $h = H/H^*$, and a prime denotes differentiation with respect to the dimensionless variable z . In addition, we have used the abbreviation

$$\gamma = (2K_2)^{-1}(K_1 + K_3), \quad (12)$$

which reduces to 1 in the weak-coupling limit. The problem now consists in minimizing the total free energy

$$\langle F \rangle = \int_{-1/2}^{1/2} dz F(z), \quad (13a)$$

with respect to θ, ϕ, S , subject to the homogeneous boundary conditions

$$\theta(\pm \frac{1}{2}) = \phi(\pm \frac{1}{2}) = S'(\pm \frac{1}{2}) = 0. \quad (13b)$$

Note first that Eq. (11) contains the function $S(z)$ only as the derivative $S'(z)$, and the corresponding Euler-Lagrange equation is easily solved to give⁸

$$S'(z) = \gamma q \sin \theta \cos \theta (1 + \gamma \sin^2 \theta)^{-1}, \quad (14)$$

which automatically satisfies the boundary conditions. The stationary nature of $\langle F \rangle$ then permits direct substitution of (14) into (11), yielding the simpler free-energy density

$$F = \text{const} + g_D \Delta^2 f, \quad (15a)$$

where^{8,9}

$$\begin{aligned} f = w^{-2} [& 2q^2(1 + \gamma)(1 + \gamma \sin^2 \theta)^{-1} + (\theta')^2(1 + 2\gamma \cos^2 \theta) \\ & + 2(\phi')^2(1 + \gamma \sin^2 \theta)] \\ & + 2h^2 \cos^2(\psi - \phi) - 2 \cos^2(\theta - \phi) \end{aligned} \quad (15b)$$

is dimensionless. Here, the three terms represent the kinetic energy, the magnetic energy, and the dipole energy, respectively.

The physical current densities are readily evaluated with the assumed order parameter (9). Use of Eq. (14) reduces the particle current to

$$\vec{J}(z) = \frac{4\Delta^2}{\hbar} \left[2K_2 Q \left(\frac{1 + \gamma}{1 + \gamma \sin^2 \theta} \right) \hat{y} - \frac{K_1}{W} \cos \theta \theta' \hat{x} \right], \quad (16)$$

where z is again dimensionless. This expression shows that the current flows predominantly along \hat{y} , but with an extra component (first noted by de Gennes and Rainer⁸) along \hat{x} , associated with the bending of \hat{l} . This last term averages to zero across the channel, because of the boundary condition on θ . Thus, the transverse flow does not affect the net transport of particles; nevertheless, an experimental search for such a contribution would be most interesting because it depends only on K_1 instead of the combination $K_1 + K_3$. Such behavior seems to provide a counterexample to the assumed equivalence of free-energy densities differing only by partial integrations.⁷ The calcula-

tion of the spin current is similar, involving contributions of the form $(\hat{d}' \times \hat{d})_\lambda$, which vanishes except for $\lambda = x$. In this way we obtain the i th component of the current for the x component of spin

$$J_{xi}^s = (4K_2 \Delta^2 / W) \phi' [(1 + \gamma \sin^2 \theta) \hat{z} - \gamma \sin \theta \cos \theta \hat{y}]_i, \quad (17)$$

which arises from the bending of \hat{d} . As expected, J_{xz}^s vanishes at the walls because of the boundary condition on ϕ' .

III. HYDRODYNAMIC FLOW

The previous general analysis will now be specialized to pure hydrodynamic flow with no magnetic field. Even in this case, however, the nonlinear coupled Euler-Lagrange equations for θ and ϕ are intractable, and we therefore make the additional approximation of small bending ($|\theta|, |\phi| \ll 1$). If $q = 0$ (no flow), then Eq. (15) for $h = 0$ attains its minimum for $\theta = \phi = 0$, with $\hat{d} \parallel \hat{l}$ owing to the dipole coupling. As q increases from zero, we expect the approximation of small deformations to remain valid; it will permit us to locate the boundary of instability in the WQ plane, separating a uniform configuration ($\theta = \phi = 0$) from one with \hat{l} and \hat{d} both tipped toward the flow direction. An expansion of Eq. (15) with $h = 0$ to second order in θ, ϕ yields

$$\begin{aligned} f = w^{-2} [& 2q^2(1 + \gamma) - 2q^2 \gamma (1 + \gamma) \theta^2 + (\theta')^2(1 + 2\gamma) \\ & + 2(\phi')^2] - 2 + 2(\theta - \phi)^2, \end{aligned} \quad (18)$$

which constitutes a quadratic form in the variables θ, ϕ .

A. Variational approximation

Although this particular problem has an exact solution, we ultimately are interested in other geometrical configurations (for example, a cylindrical pore) that will require approximations. Consequently, it is valuable to analyze even the slab with such techniques, for comparison with the exact results can then indicate the accuracy of the approximations. In the present case, we shall use a variational method. The symmetry of the system suggests that θ, ϕ in the lowest deformed state will be even functions of z ; otherwise, the node at the center would imply additional kinetic energy of bending. It is convenient to expand $\theta(z)$ in a complete set of even functions that satisfy the boundary conditions (13b),

$$\theta(z) = \sum_n A_n \cos[(2n + 1)\pi z], \quad (19)$$

where the sum on n starts at zero. In principle, $\phi(z)$ could be expanded in a similar series, but it is preferable to follow Chandrasekhar,¹⁶ and ex-

plicitly solve the Euler-Lagrange equation

$$\phi'' - w^2\phi = -w^2\theta. \quad (20)$$

Here, the right-hand side is interpreted as an inhomogeneous term, and the linearity permits an expansion in the form

$$\phi(z) = \sum_n A_n \phi_n(z), \quad (21)$$

where ϕ_n satisfies the equation

$$\phi_n'' - w^2\phi_n = -w^2 \cos[(2n+1)\pi z], \quad (22)$$

and the boundary conditions $\phi_n'(\pm \frac{1}{2}) = 0$. These functions are readily determined to be

$$\begin{aligned} \phi_n(z) = & \frac{w^2}{w^2 + \pi^2(2n+1)^2} \\ & \times \left(\frac{(-1)^n \pi(2n+1) \cosh(wz)}{w \sinh[(1/2)w]} + \cos[(2n+1)\pi z] \right), \end{aligned} \quad (23)$$

which, in effect, already incorporates half the solution. As a result, the subsequent analysis involves only the single set of coefficients $\{A_n\}$.

The remaining problem is the evaluation of the total free energy $\langle f \rangle$ for the functions (19) and (21). A straightforward calculation eventually gives

$$\langle f \rangle = 2q^2 w^{-2}(1+\gamma) - 2 + \sum_{mn} c_{mn} A_m A_n, \quad (24)$$

where m and n start from zero and

$$\begin{aligned} c_{mn} = & \delta_{mn} \left(\frac{\pi^2(2n+1)^2}{w^2 + \pi^2(2n+1)^2} \right. \\ & + \frac{1+2\gamma}{2w^2} \pi^2(2n+1)^2 - \frac{q^2\gamma(1+\gamma)}{w^2} \Big) \\ & - \frac{4w \coth[(1/2)w] (-1)^{m+n} \pi^2(2m+1)(2n+1)}{[w^2 + \pi^2(2m+1)^2][w^2 + \pi^2(2n+1)^2]} \end{aligned} \quad (25)$$

$$Q_c^2 \approx W^{-2} \times \begin{cases} \frac{\pi^2(1+2\gamma)}{2\gamma(1+\gamma)} + \frac{W^2}{\gamma(1+\gamma)L^{*2}} \left(1 - \frac{8}{\pi^2} \right), & W \ll L^* \\ \frac{\pi^2(3+2\gamma)}{2\gamma(1+\gamma)} \left(1 - \frac{8L^*}{W(3+2\gamma)} \right), & W \gg L^*. \end{cases} \quad (28a)$$

Note the relative constancy of $Q_c W$, implying that the critical velocity $v_c = \hbar Q_c / 2m_3$ varies essentially inversely with the channel width W , keeping the product $v_c W$ of order \hbar/m_3 . In the limit of small w , Eq. (28a) reproduces the expression found by de Gennes and Rainer,⁸ who neglected the dipole energy and (in effect) took $\phi = 0$. This correspondence reflects the dominance of the kinetic energy

is symmetric under interchange of its indices. Note that $\langle f \rangle$ contains a quadratic form in $\{A_n\}$. If this contribution is positive definite, then the equilibrium configuration is uniform; conversely, the uniform state becomes unstable with respect to a deformed one whenever $\{c_{mn}\}$ ceases to be positive definite.

Equation (24) provides a variational principle for the equilibrium configuration, and the trial function can be systematically improved by increasing the number of coefficients. The simplest approximation retains only A_0 , in which case

$$\langle f \rangle = 2q^2 w^{-2}(1+\gamma) - 2 + c_{00} A_0^2. \quad (26)$$

Evidently, the equilibrium value of A_0 vanishes whenever $c_{00} > 0$; if c_{00} becomes negative, however, then $\langle f \rangle$ is unbounded from below, and $|A_0|$ increases indefinitely. This last situation represents the failure of our expansion to second order in θ and ϕ , since nonlinearities become significant. In the present approximation, we see that the condition $c_{00} = 0$ characterizes the onset of instability. Setting $m = n = 0$ in (25) yields the condition

$$\begin{aligned} q_c^2 \equiv Q_c^2 W^2 = & \frac{\pi^2(1+2\gamma)}{2\gamma(1+\gamma)} + \frac{\pi^2 w^2}{\gamma(1+\gamma)(w^2 + \pi^2)} \\ & - \frac{4w^3 \pi^2 \coth[(1/2)w]}{\gamma(1+\gamma)(w^2 + \pi^2)^2}. \end{aligned} \quad (27)$$

With increasing flow in a fixed channel of width $W = wL^*$, the uniform state remains stable up to a critical value $Q_c = q_c/W$, at which point \hat{l} tilts away from its original \hat{z} direction through a small angle $\theta(z) = A_0 \cos(\pi z/W)$; in addition, the dipole energy couples the directions of \hat{l} and \hat{d} , tilting \hat{d} through the angle $A_0 \phi_0(z)$. The present approximation fixes only the form of these functions; a determination of A_0 would require higher corrections to Eq. (18).

The critical flow rate in (27) has a simple form for small and large channels:

for narrow channels. In the opposite limit of wide channels, however, the dipole energy is important nearly everywhere, producing extra curvature energy associated with the bending of \hat{d} . The intermediate regime $W \approx L^*$ is experimentally accessible, and measurements of v_c in channels with widths spanning this value might determine γ in Eq. (12).

B. Exact solution

The approximate free energy $\langle f \rangle$ in (18) has the Euler-Lagrange equations

$$\theta'' = (1 + 2\gamma)^{-1} [2w^2 - 2q^2\gamma(1 + \gamma)]\theta - 2w^2(1 + 2\gamma)^{-1}\phi, \quad (29a)$$

$$\phi'' = w^2\phi - w^2\theta, \quad (29b)$$

which must be combined with the boundary conditions (13b). For general w and q , no solutions exist, leading to an eigenvalue problem for the dimensionless parameter q_c in a channel of fixed dimensionless width w . The solutions may be classified as even or odd, and each set has an infinite sequence of eigenfunctions and eigenvalues, with the n th even (odd) solution signalling the appearance of an orientational instability to an even (odd) state with n nodes. Similar behavior has been studied in $^3\text{He-B}$ by Fomin and Vuorio.¹⁵ As noted previously, the first instability is expected to yield an even deformation, and only such solutions are considered here.

Equations (29) have constant coefficients, which allows a direct solution in exponential form θ , $\phi \propto e^{\mu z}$. Substitution into (29) yields the consistency relation

$$\mu^4 - \mu^2(1 + 2\gamma)^{-1}[(3 + 2\gamma)w^2 - 2q^2\gamma(1 + \gamma)] - 2q^2w^2\gamma(1 + \gamma)(1 + 2\gamma)^{-1} = 0, \quad (30)$$

which can be solved directly for the two roots μ_{\pm}^2 . Since the product $\mu_+^2\mu_-^2$ is negative, it is convenient to redefine them as $\mu_+ = \mu$, $\mu_- = i\nu$, and the corresponding even solutions become

$$\begin{aligned} \theta(z) &= (1 - \mu^2/w^2)A \cosh \mu z + (1 + \nu^2/w^2)B \cos \nu z, \\ \phi(z) &= A \cosh \mu z + B \cos \nu z. \end{aligned} \quad (31)$$

Application of the boundary conditions then gives the desired eigenvalue equation

$$\mu^{-1}(\mu^2 - w^2) \coth(\frac{1}{2}\mu) = \nu^{-1}(\nu^2 + w^2) \cot(\frac{1}{2}\nu). \quad (32)$$

The lowest root fixes the instability to an even deformed state with no nodes, and higher ones include successively more oscillations.

Equation (32) is a transcendental equation, and explicit determination of q_c requires numerical analysis. Thus we first examine a few limiting cases, where analytic expressions can be found. If $w \rightarrow 0$, an expansion in powers of w precisely reproduces the variational approximation [Eq. (28a)]; for $w \rightarrow \infty$, moreover, the exact result differs from (28b) only in the correction term, where the factor $(3 + 2\gamma)$ is replaced by $[(3 + 2\gamma)(1 + 2\gamma)]^{1/2}$. In these limits, at least, the variational approximation seems remarkably accurate, and detailed evaluation of (32) confirms this behavior for all

w . Figure 1 plots the slowly varying product $q_c = Q_c W$ against $w = W/L^*$, with $\gamma = 1$. As noted previously, this curve represents a transition to the lowest even state, but the boundary for transitions to odd states should have a similar shape, but displaced upward. On the present scale, the variational approximation (27) is indistinguishable from the exact expression.

To conclude this section, we consider the current densities for these two states. The uniform configuration has a constant current density $(8K_2\Delta^2/\hbar)Q(1 + \gamma)\hat{y}$, with no spin current. On the other hand, the deformed state is considerably more complicated. To first order in θ and ϕ , J_y remains unchanged, but the bending of \hat{l} induces a small transverse flow $J_x = -(4K_1\Delta^2/\hbar W)\theta'$ that changes sign at $z = 0$. In more physical configurations, like axial flow in a cylindrical tube, this transverse flow would presumably become a circulating current about the symmetry axis. The deformed state in a slab also carries a weak-spin current $J_{xz}^s = (4K_2\Delta^2/W)\phi'$ that changes sign at $z = 0$. This flow transports the x component of spin towards or away from the center of the channel, with spin conservation ensured by the "internal Josephson effect," as discussed by Fomin and Vuorio.¹⁵

IV. UNIFORM MAGNETIC FIELD

The vector \hat{l} played a dominant role in the preceding example of hydrodynamic flow, for it experiences direct perturbations both from the surface and from the macroscopic velocity field. On the other hand, the spin vector \hat{d} senses the hydrodynamic flow only indirectly through the dipole energy. The situation changes markedly if the flow is replaced by a magnetic field, which affects \hat{d}

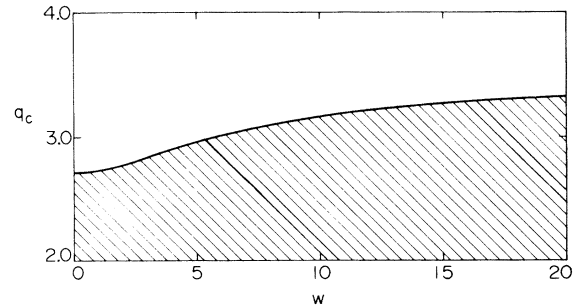


FIG. 1. Critical value of the product $q_c \equiv Q_c W \equiv 2m_3 v_c W/\hbar$ for a hydrodynamically induced orientational transition of $^3\text{He-A}$ from a uniform state (shaded) to a deformed one (unshaded) in a channel of width W . Here, $w = W/L^*$, with $L^* \approx 6 \times 10^{-4}$ cm, and $\gamma = 1$. The curve was determined either from the exact eigenvalue equation (32), or from the variational approximation (27).

directly, tending to align it perpendicular to \vec{H} . If \vec{H} lies along \hat{y} , then the configuration $\hat{l} \parallel \hat{d} \parallel \hat{z}$ minimizes both the magnetic energy and the dipole energy. For other orientations, however, competing effects act on \hat{d} , and only a detailed study can determine the equilibrium state. Ambegaokar and Rainer⁹ have performed such a calculation for $\vec{H} \parallel \hat{z}$, and we here extend the analysis to a tipped magnetic field $\vec{H} = H(\hat{y} \sin\psi + \hat{z} \cos\psi)$ lying in the yz plane at an angle ψ from \hat{z} . Although this modest generalization complicates the algebra considerably, it predicts that many physical properties (like the shape of the phase boundary for orientational transitions) depend qualitatively on ψ .

The problem of interest is to obtain the equilibrium configuration of $^3\text{He-A}$ in a slab geometry by minimizing the free-energy density (15), with $q=0$. The simplest state that satisfies the boundary conditions is strictly uniform, with $\hat{l} \parallel \hat{z}$ and \hat{d} tipped in the yz plane at a constant angle Φ . The equation $\partial f / \partial \Phi = 0$ yields the solution

$$\cos 2\Phi = \kappa^{-2}(1 - h^2 \cos 2\psi), \quad (33a)$$

$$\sin 2\Phi = -\kappa^{-2}h^2 \sin 2\psi, \quad (33b)$$

where

$$\kappa^4 = 1 - 2h^2 \cos 2\psi + h^4 \quad (34)$$

is nonnegative. These relations confirm that \hat{d} lies along \hat{z} for \vec{H} along \hat{y} . More interesting is the case \vec{H} along \hat{z} , when \hat{d} changes discontinuously from \hat{z} to \hat{y} as H increases through $H^* \approx 25$ Oe. A similar but continuous transition occurs for other ψ , with \hat{d} rotating from \hat{z} to $\hat{x} \times \hat{H}$ with increasing field.

To study the possibility of an orientational transition in a uniform tipped magnetic field, consider small deviations from the uniform state, with

$$\phi_n(z) = \frac{w^2 \cos 2\Phi}{\kappa^2 w^2 + \pi^2 (2n+1)^2} \left(\frac{(-1)^n \pi (2n+1) \cosh(\kappa w z)}{\kappa w \sinh[(1/2)\kappa w]} + \cos[(2n+1)\pi z] \right), \quad (38)$$

which also follows from (23).

The evaluation of the free energy per unit area $\langle f \rangle$ is straightforward and eventually gives

$$\langle f \rangle = h^2 - 1 - \kappa^2 + \sum_n b_n A_n + \sum_{mn} c_{mn} A_m A_n, \quad (39)$$

where

$$b_n = -4\pi^{-1} \sin(2\Phi) (-1)^n (2n+1)^{-1} \quad (40a)$$

and

$$c_{mn} = \delta_{mn} \left(\frac{(1+2\gamma)\pi^2 (2n+1)^2}{2w^2} + \cos 2\Phi - \frac{w^2 \cos^2 2\Phi}{\kappa^2 w^2 + \pi^2 (2n+1)^2} \right) - \frac{4w^2 (\cos^2 2\Phi) (\kappa w)^{-1} \coth(\frac{1}{2}\kappa w) (-1)^{m+n} \pi^2 (2m+1)(2n+1)}{[\kappa^2 w^2 + \pi^2 (2m+1)^2][\kappa^2 w^2 + \pi^2 (2n+1)^2]}. \quad (40b)$$

The linear term in (39) occurs whenever the magnetic field is tipped from \hat{y} or \hat{z} . For definiteness, suppose ψ is negative; Eqs. (33b) and (40a) then imply that b_0 is also negative. Independent of the

$|\theta| \ll 1$ and $|\phi - \Phi| = |\bar{\phi}| \ll 1$. An expansion to second order in the small quantities θ and $\bar{\phi}$ yields

$$f = h^2 - 1 - \kappa^2 - 2\theta \sin 2\Phi + w^{-2}[(\theta')^2(1+2\gamma) + 2(\phi')^2] - 2h^2 \cos(2\Phi - 2\psi)\phi^2 + 2\cos(2\Phi)(\phi - \theta)^2, \quad (35)$$

where the bar on ϕ has been omitted for simplicity. Note the presence of a linear term in θ , which implies that the system can always lower its free energy by undergoing a small deformation whenever $\sin 2\Phi \neq 0$. If the quadratic contributions are positive definite, however, the equilibrium state remains "quasiuniform" with θ and ϕ remaining small; otherwise, the state undergoes large deformations. The problem then is to determine the boundary in the WH plane where $\langle f \rangle$ ceases to be bounded from below with increasing θ or ϕ .

A. Variational approximation

Before presenting an exact solution for the phase boundary, we again apply the variational method from Sec. III A. This approach is algebraically simpler than the exact one; it also clarifies the new physical phenomena induced by tilting the magnetic field. The symmetry of the problem suggests an even solution, and we accordingly take $\theta(z)$ in the form (19). Use of (34) reduces the Euler-Lagrange equation for ϕ to

$$\phi'' - \kappa^2 w^2 \phi = -w^2 \cos(2\Phi) \theta, \quad (36)$$

again implying an expansion of the form (21), but with ϕ_n now satisfying

$$\phi_n'' - \kappa^2 w^2 \phi_n = -w^2 \cos(2\Phi) \cos[(2n+1)\pi z]. \quad (37)$$

An elementary calculation leads to

quadratic parts of (39), the choice $A_0 = 0$ can never minimize the free energy, for $\langle f \rangle$ initially decreases linearly with increasing A_0 . Consequently, the strictly uniform state ($A_n = 0$ for all n) is never

favorable for ${}^3\text{He-A}$ in a slab with a tipped magnetic field (unless $\sin 2\psi = 0$). Instead, the field acts on \hat{d} in the bulk fluid, bending it away from the uniform orientation Φ , making it more nearly perpendicular to \hat{H} . Simultaneously, the dipole coupling bends \hat{l} away from \hat{z} and \hat{H} .

The existence of such deformations immediately raises the question of their stability, which may be answered by considering the quadratic terms in (39). If they are positive definite, then $\langle f \rangle$ has a true minimum for some set of finite coefficients; conversely, an instability occurs whenever the quadratic terms cease to be positive definite. This criterion, which does not involve the linear terms, is precisely that used in Sec. III A.

To illustrate the preceding remarks, consider the simple trial function $A_0 \neq 0, A_1 = A_2 = \dots = 0$. For positive c_{00} , the free energy $\langle f \rangle$ has the minimum value

$$\langle f \rangle_{\min} = h^2 - 1 - \kappa^2 - b_0^2/4c_{00} \quad (41)$$

occurring at

$$(A_0)_{\min} = -b_0/2c_{00}. \quad (42)$$

If c_{00} becomes small as h and w vary, the equilibrium state becomes increasingly deformed; in particular, the condition $c_{00} = 0$ characterizes the onset of instability, which here takes place at

$$\frac{(1+2\gamma)\pi^2}{2w^2} + \cos 2\psi = w^2 \cos^2 2\psi \times \left(\frac{1}{\kappa^2 w^2 + \pi^2} + \frac{4\pi^2 \coth(\frac{1}{2}\kappa w)}{\kappa w(\kappa^2 w^2 + \pi^2)^2} \right). \quad (43)$$

This equation determines the phase boundary in the wh plane separating the quasiuniform state with bounded deformations from one involving large-amplitude bending.

It is valuable to investigate the detailed form of the phase boundary predicted in Eq. (43).

(i) If $h \rightarrow 0$, an expansion of (33), (34), and (43) yields the explicit relation

$$h^2 \cos 2\psi \approx \pi^2 w^{-2} (3 + 2\gamma), \quad (44)$$

showing that the critical field for an orientational transition varies inversely with w for large w ; in addition, no transition can occur unless $\cos 2\psi \geq 0$ (namely, $|\psi| \leq \frac{1}{4}\pi$). If the latter condition holds, an experimental determination of the product hw along the phase boundary as $h \rightarrow 0$ could provide an alternative means of measuring γ .

(ii) If $h \rightarrow \infty$, the critical field is given approximately by

$$(1/2)(1+2\gamma)\pi^2 w^{-2} \approx \cos 2\psi + h^{-2} \cos 4\psi. \quad (45)$$

This equation identifies a characteristic channel width $w_0 = \pi[\frac{1}{2}(1+2\gamma)/\cos 2\psi]^{1/2}$, with the quasiuniform state stable at high fields for $w < w_0$. Moreover, the critical-field curve for large h approaches w_0 from smaller or larger values of w , determined according to whether $\cos 4\psi$ is positive or negative.

(iii) For $w \rightarrow \infty$, an expansion of (43) leads to the implicit relation for the critical field

$$\pi^2 w^{-2} [\frac{1}{2} + \gamma + \kappa^{-8}(1 - h^2 \cos 2\psi)^2] = \kappa^{-6} h^2 (1 - h^2 \cos 2\psi)(\cos 2\psi - h^2). \quad (46)$$

Since the left-hand side is small and positive (of order w^{-2}), solutions exist only if one of the three factors on the right-hand side is also small. The first possibility ($h \rightarrow 0$) has already been analyzed, and the remaining two require that the product $(1 - h^2 \cos 2\psi)(\cos 2\psi - h^2)$ be positive. No solutions exist in the range

$$\cos 2\psi \leq h^2 \leq \sec 2\psi, \quad (47)$$

where the quasiuniform state remains absolutely stable. As h^2 approaches these limiting values from below and above, respectively, the critical field curves move toward large w ; the only exception is at $\psi = 0$ ($\hat{H} \parallel \hat{z}$), when the critical-field curve actually reaches $w = 0$ at $h = 1$. This last case, which was examined by Ambegaokar and Rainer,⁹ also follows from (43) with a suitable limiting procedure.

The preceding discussion indicates that a tipped magnetic field significantly affects the location of the orientational transition in the wh plane. Owing to the linear term in (35), tipping the field also tends to smear the transition, because [compare (42)] the texture is somewhat deformed in any finite field. To estimate this effect, we may augment the free-energy density with a cubic term, leading to the approximate form

$$\langle f \rangle = \langle f_0 \rangle + b_0 A_0 + c_{00} A_0^2 + d_0 A_0^3.$$

For small h , the previously calculated b_0 has the order-of-magnitude $h^2 \sin 2\psi$, which properly vanishes at $h = 0$ and for $\psi = 0^\circ$ or 90° ; we assume a similar value $d_0 \approx -\lambda h^2 \sin 2\psi$, with λ a numerical constant of order unity. Minimization of this $\langle f \rangle$ near the critical field h_c [given in Eq. (44)] yields the approximate equilibrium amplitude

$$(A_0)_{eq} = \frac{-\frac{1}{2} h_c \sin 2\psi}{(h_c - h) \cos 2\psi + [(h_c - h)^2 \cos^2 2\psi + \frac{3}{4} \lambda h_c^2 \sin^2 2\psi]^{1/2}},$$

where the limit $\lambda=0$ represents the omission of the cubic term in $\langle f \rangle$. Evidently, the transition has a width Δh of order $h_c \tan 2\psi$, which is small for nearly perpendicular fields, but becomes large near $\psi \approx 45^\circ$. Whenever $\tan 2\psi \leq 1$, the equilibrium deformation grows rapidly from a small value to one of order unity as h passes through the region $|h_c - h| \leq h_c \tan 2\psi$. The present formalism assumes small deformations, however, which precludes a more detailed study of the transition. An improved treatment must rely on the full nonlinear free energy in (15b); this question is currently under investigation.

To illustrate the expected behavior, Fig. 2 shows the wh plane with the phase boundary separating the two phases at three distinct values of ψ . Note that the critical field need not be a single-valued function of w , but the inverse function always gives a unique critical width for a given value of h . These figures indicate that a perpendicular field ($\psi=0$) is atypical in several ways. First, its phase boundary lies farthest to the left, maximizing the region of instability. Second, the quasiuniform state is stable for all w throughout the finite range of field given in (47). Finally, a detailed examination confirms that the quasiuniform state remains stable for all h and w if $\cos 2\psi < 0$. This latter region includes the special case of parallel field ($\psi = \frac{1}{2}\pi$), when the equilibrium state $\hat{l} \parallel \hat{d} \parallel \hat{z}$ follows by inspection.

B. Exact solution

The exact solution for the phase boundary in the wh plane is similar to, but more complicated than that in Sec. III B for the hydrodynamic instability. The free-energy density (35) has the Euler-Lagrange equations

$$\theta'' = (1+2\gamma)^{-1} [2w^2(\cos 2\Phi)(\theta - \phi) - w^2 \sin 2\Phi], \quad (48a)$$

$$\phi'' = w^2 \kappa^2 \phi - w^2(\cos 2\Phi)\theta, \quad (48b)$$

$$0 = \mu^4 - \mu^2 [\kappa^2 w^2 + (1+2\gamma)^{-1} 2w^2 \cos 2\Phi] + (1+2\gamma)^{-1} 2w^4 \cos 2\Phi (\kappa^2 - \cos 2\Phi). \quad (49)$$

The product $\cos 2\Phi(\kappa^2 - \cos 2\Phi)$ may be rewritten $h^2 \kappa^{-4} (1 - h^2 \cos 2\psi)(h^2 - \cos 2\psi)$, showing that the product of the roots $\mu_+^2 \mu_-^2$ is negative for $0 < h^2 < \cos 2\psi$, or for $0 < \sec 2\psi < h^2$. If we again introduce the notation $\mu = \mu_+$, $i\nu = \mu_-$, and apply the boundary conditions on θ and ϕ , the general even solution to (48) becomes

$$\theta(z) = (\kappa^2 w^2 - \mu^2) A \cosh \mu z + (\kappa^2 w^2 + \nu^2) B \cos \nu z + (\kappa^2 - \cos 2\Phi)^{-1/2} \kappa^2 \tan 2\Phi, \quad (50a)$$

$$\phi(z) = w^2 \cos 2\Phi (A \cosh \mu z + B \cos \nu z) + (\kappa^2 - \cos 2\Phi)^{-1/2} \sin 2\Phi, \quad (50b)$$

where

$$\begin{aligned} \mu \sinh(\tfrac{1}{2} \mu) A &= \nu \sin(\tfrac{1}{2} \nu) B \\ &= -\frac{1}{2} \frac{\kappa^2 \tan 2\Phi}{(\kappa^2 - \cos 2\Phi) [(\nu^2 + \kappa^2 w^2) \nu^{-1} \cot(\tfrac{1}{2} \nu) - (\mu^2 - \kappa^2 w^2) \mu^{-1} \coth(\tfrac{1}{2} \mu)]}. \end{aligned} \quad (51)$$

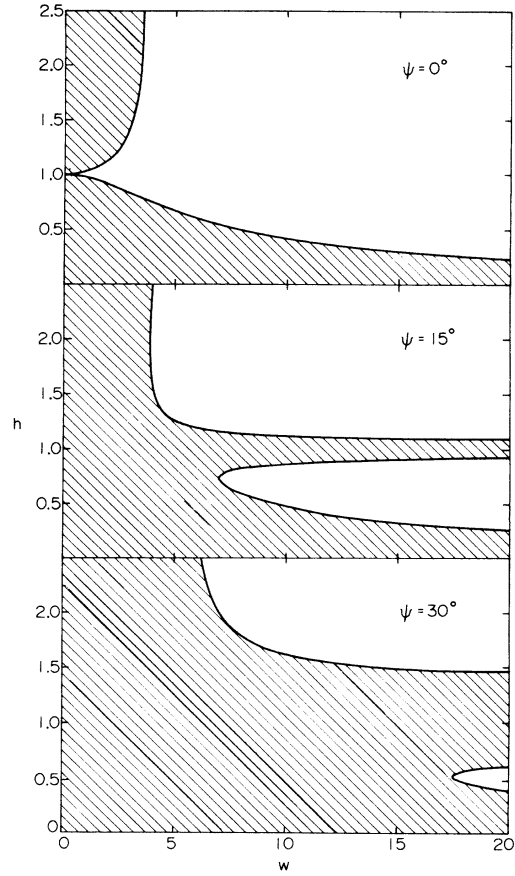


FIG. 2. Phase boundary in the wh plane separating a quasiuniform state of ${}^3\text{He-A}$ (shaded) from a deformed one (unshaded) for various tipping angles ψ between \hat{H} and \hat{z} . Here, $w = W/L^*$, with $L^* \approx 6 \times 10^{-4}$ cm, $h = H/H^*$, with $H^* \approx 25$ Oe, and $\gamma = 1$. The curves were determined either from the exact eigenvalue equation (52) or the variational approximation (43).

which have been simplified slightly with Eqs. (33) and (34). This set of second-order differential equations has solutions of the form $\theta, \phi \propto e^{\mu z}$, with

Whenever the coefficients A and B are bounded, then the inhomogeneous term fixes the whole solution, exactly as in the variational approximation, with $A_0 \neq 0$. This behavior represents the quasi-uniform state, with the tipped field inducing a slight departure from strict uniformity. As the parameters w and h vary, however, the last factor in the denominator of (51) can vanish, leading to an orientational instability at the phase boundary determined by the transcendental equation

$$(\mu^2 - \kappa^2 w^2) \mu^{-1} \coth(\tfrac{1}{2}\mu) = (\nu^2 + \kappa^2 w^2) \nu^{-1} \cot(\tfrac{1}{2}\nu). \quad (52)$$

This equation turns out to have no solutions if $\cos 2\psi < 0$, or if h^2 lies in the range (47), indicating that the quasiuniform state is absolutely stable in these cases. Moreover, rather tedious expansions reproduce the several limits obtained previously in Sec. IV A with variational methods. Finally, numerical evaluation for $\gamma = 1$ and certain selected ψ yields the curves in Fig. 2, which are indistinguishable from the variational phase boundaries obtained from Eq. (43). Once again, the variational approximation is seen to be remarkably accurate.

To conclude this section, we may note that even the quasiuniform state generally involves bending of the unit vector \hat{d} . Consequently, despite the absence of particle currents, such textures in tipped

magnetic fields carry spin currents like those discussed at the end of Sec. III. A similar situation in ${}^3\text{He-B}$ has been studied by Fomin and Vuorio.¹⁵

V. COMBINED HYDRODYNAMIC FLOW AND TIPPED MAGNETIC FIELD

Actual experiments on hydrodynamic flow in ${}^3\text{He-A}$ will often involve a magnetic field, for example, to provide the static field for NMR studies.¹⁷ Hence, it is interesting to consider the combined effect of a uniform hydrodynamic flow $\vec{v} = \hbar Q \hat{y} / 2m_3$, and an external uniform magnetic field tipped at an angle ψ in the yz plane to the normal \hat{z} . As in the previous section, the unperturbed uniform solution is given by (33), with $\theta = 0$ and $\phi = \Phi$. In the presence of hydrodynamic flow, the dimensionless free energy (35) is augmented by a term $2q^2 w^{-2}(1 + \gamma)(1 - \gamma\theta^2 + \dots)$, and the critical curve again can be determined either variationally or exactly; for simplicity, only the variational approximation will be considered here. The trial functions (19), (21), and (38) continue to apply, with the one new feature that c_{mn} in Eq. (40b) acquires an additional term $-\delta_{mn} q^2 \gamma (1 + \gamma) w^{-2}$. If we retain only the term A_0 in the expansion of θ and ϕ , the approximate condition $c_{00} = 0$ implicitly determines the onset of the orientational transition. It is convenient to consider \vec{H} fixed, interpreting the resulting expression

$$q_c^2 \equiv Q_c^2 W^2 = \frac{1}{\gamma(\gamma+1)} \left[\frac{1}{2} \pi^2 (1 + 2\gamma) + w^2 \cos 2\Phi \left(1 - \frac{w^2 \cos 2\Phi}{\kappa^2 w^2 + \pi^2} \right) - \frac{4w^3 \pi^2}{\kappa} \frac{\cos^2(2\Phi) \coth[(1/2)\kappa w]}{(\kappa^2 w^2 + \pi^2)^2} \right] \quad (53)$$

to give the critical flow velocity $v_c = \hbar Q_c / 2m_3$ in a slab of width $W = wL^*$ subject to a tipped magnetic field $H = hH^*$. Equation (53) evidently reduces to (27) when $h = 0$ (and hence $\kappa = \cos 2\Phi = 1$); for a specified tipping angle ψ , it is meaningful only in the shaded portions of Fig. 2, because otherwise the orientational transition already occurs for stationary fluid ($q = 0$). In particular, it should apply for all h and w if $|\psi| > 45^\circ$, with the transition increasingly sharp as the field becomes parallel to the flow.

The implications of Eq. (53) are most readily appreciated by examining the limiting behavior for narrow and wide channels. A straightforward expansion yields

$$Q_c^2 \approx \begin{cases} \frac{\pi^2(1+2\gamma)}{2W^2\gamma(1+\gamma)} \left[1 + O\left(\frac{W^2}{L^{*2}}\right) \right], & W \ll L^* \\ \frac{h^2(1-h^2\cos 2\psi)(h^2 - \cos 2\psi)}{L^{*2}\gamma(1+\gamma)(1-2h^2\cos 2\psi+h^4)^{3/2}} \\ \times \left[1 + O\left(\frac{L^{*2}}{W^2}\right) \right], & W \gg L^* \end{cases} \quad (54)$$

which should be compared with Eq. (28). As suggested by physical considerations, the magnetic field has little effect for narrow channels, because the kinetic energy predominates; thus the corresponding critical velocity $v_c = (\pi\hbar/2m_3W)[(1+2\gamma)/2\gamma(1+\gamma)]^{1/2}$ varies inversely with W , independent of the field. On the other hand, Q_c and v_c approach constant, but field dependent values for large $W \gg L^*$:

$$v_c \approx \frac{\hbar}{2m_3L^*} \left[\frac{h^2(1-h^2\cos 2\psi)(h^2 - \cos 2\psi)}{\gamma(1+\gamma)(1-2h^2\cos 2\psi+h^4)^{3/2}} \right]^{1/2}. \quad (55)$$

This expression is well defined whenever the quantity in large brackets is positive, which always holds for $|\psi| > 45^\circ$ (namely, \vec{H} lying within 45° of the direction $\pm \hat{v}$). Moreover, it vanishes for $h = 0$, leaving only the correction term which then reproduces the previous inverse relation (28b) between Q_c and W . The transition should be sharp for \vec{H} parallel to the flow, and (55) predicts that the corresponding v_c for wide channels grows monotonically as $h(1+h^2)^{-1/2}$ with increasing h .

Figure 3 illustrates this behavior for various fixed field strengths. Similar field dependence occurs for all $|\psi| > 45^\circ$. The dimensional coefficient in (55) has the numerical value $\approx 0.17 \text{ cm sec}^{-1}$, and the second factor is less than 1. Taking, for example, $H = 25 \text{ Oe}$ and $\psi = 90^\circ$, we find $v_c \approx 0.08 \text{ cm sec}^{-1}$.

VI. DISCUSSION

This paper has analyzed the simplest type of orientational transitions in superfluid ^3He —those of the *A* phase confined between parallel planes of constant z . As in other more complicated cases, the possibility of transitions between various textures arises from a competition between various orientational perturbations that act on \hat{l} and \hat{d} . Transitions of the sort considered here might be detectable through NMR. In particular, the quasi-uniform state should produce a narrow resonance line that broadens on passing into the deformed configuration, because of the separate resonances associated with the spatially nonuniform orientations of \hat{l} and \hat{d} .^{18,19}

Hydrodynamic flow provides the most straightforward example.⁸ In narrow channels with width $W \ll L^* \approx 6 \times 10^{-4} \text{ cm}$, the kinetic energy of curvature opposes the tendency for \hat{l} to lie along the flow direction, leading to a critical velocity of the form $v_c \propto \hbar/m_3 W$. As W becomes larger, however, the dipole coupling between \hat{d} and \hat{l} also plays a role, increasing the numerical value of the product $v_c W$, but leaving the essential form unchanged. An experimental study of such effects might determine the ratio $\gamma = (K_1 + K_3)/2K_2$ of constants that appear in the kinetic energy density.

From a mathematical point of view, a hydrodynamic flow with wave number \vec{Q} and a magnetic field \vec{H} couple to the axial state in similar ways, involving products of the form $(\vec{H} \cdot \hat{d})^2$ and $-(\vec{Q} \cdot \hat{l})^2$. In practice, however, \vec{H} and \vec{Q} differ significantly in that \vec{Q} necessarily lies in the xy plane, whereas \vec{H} can be arbitrary. As a result, magnetic fields offer a much richer variety of textures in a bounded domain. Indeed, we find that the general situation for arbitrary tipping angle ψ of \vec{H} relative to \hat{z} is much more complex than for the special cases $\psi = 0$ and $\psi = \frac{1}{2}\pi$, which are most closely analogous to the uniform hydrodynamic flow. For example, certain values of angle ψ and field strength never

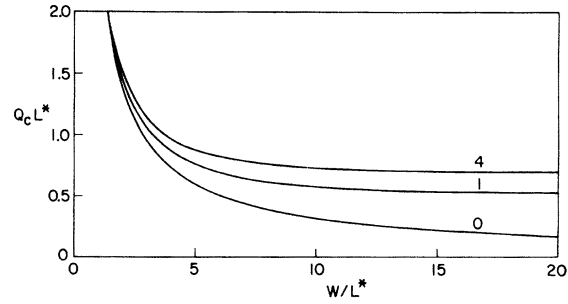


FIG. 3. Critical flow rate $Q_c L^* = 2m_3 v_c L^*/\hbar$ for an orientational transition of $^3\text{He-A}$ in a channel of width, W , subject to a magnetic field H , parallel to the flow velocity ($\psi = 90^\circ$). Here, $L^* \approx 6 \times 10^{-4} \text{ cm}$, and $\gamma = 1$. The curves, computed from (53), are labeled with the value of $h = H/H^*$, where $H^* \approx 25 \text{ Oe}$.

induce an orientational transition for any channel width W , yet other values lead to transitions over wide ranges of W . In any specific case, the qualitative behavior can be inferred from Fig. 2, which provides several distinct examples. As in the case of hydrodynamic flow, the precise location of the magnetic phase boundary depends on γ , and experimental studies of this effect again could help determine the kinetic energy density.

It is interesting to relate the present slab geometry to practical physical configurations. Most importantly, our model lacks boundaries in the transverse (x and y) directions, so that \hat{z} specifies a unique normal to the surface. In contrast, experimental geometries typically have spatially varying normals, so that a uniform applied magnetic field would act differently at different points on the boundary. One conceivable procedure to incorporate the effect of curved boundaries would be to perform an appropriate average of the expressions from Sec. IV, but this approach seems unlikely to predict the correct phase boundary in (say) a cylindrical container. As a more rigorous alternative, we are now investigating cylindrically symmetric solutions to the Ginzburg-Landau equations, where the explicit appearance of the radial variable should preclude an exact solution of the type considered in Secs. III B and IV B. Fortunately, variational techniques remain feasible, and we hope in a subsequent paper to consider orientational transitions in a cylindrical geometry.

*Supported in part by the NSF Grant No. DMR 75-08516.

¹A. J. Leggett, Rev. Mod. Phys. **47**, 331 (1975).

²J. C. Wheatley, Rev. Mod. Phys. **47**, 415 (1975).

³P. W. Anderson and P. Morel, Phys. Rev. **123**, 1911 (1961).

⁴N. D. Mermin and G. Stare, Phys. Rev. Lett. **30**, 1135 (1973).

⁵N. D. Mermin and V. Ambegaokar, in *Collective Properties of Physical Systems*, edited by B. Lundquist and S. Lundquist (Academic, New York, 1974), pp. 97-102.

- ⁶A. L. Fetter, in *Quantum Statistics and the Many-body Problem*, edited by S. B. Trickey, W. P. Kirk, and J. W. Dufty (Plenum, New York, 1975), p. 127.
- ⁷V. Ambegaokar, P. G. de Gennes, and D. Rainer, *Phys. Rev. A* **9**, 2676 (1974).
- ⁸P. G. de Gennes and D. Rainer, *Phys. Lett. A* **46**, 429 (1974).
- ⁹V. Ambegaokar and D. Rainer (unpublished); V. Ambegaokar (unpublished).
- ¹⁰G. Barton and M. A. Moore, *J. Low Temp. Phys.* **21**, 489 (1975).
- ¹¹A. J. Leggett, *Ann. Phys. (N.Y.)* **85**, 11 (1974).
- ¹²P. W. Anderson and W. F. Brinkman, *Phys. Rev. Lett.* **30**, 1108 (1973); W. F. Brinkman and P. W. Anderson, *Phys. Rev. A* **8**, 2732 (1973).
- ¹³E. I. Blount (unpublished); D. A. Dahl, Ph. D. thesis (Stanford University, 1975) (unpublished); P. Wölfle, *Phys. Lett. A* **47**, 224 (1974).
- ¹⁴P. G. de Gennes, *Phys. Lett. A* **44**, 271 (1973).
- ¹⁵I. Fomin and M. Vuorio, *J. Low Temp. Phys.* **21**, 271 (1975).
- ¹⁶S. Chandrasekhar, *Hydrodynamic and Hydromagnetic Stability* (Oxford U.P., Oxford, 1961), Secs. 15 and 17.
- ¹⁷R. M. Mueller, E. B. Flint, and E. D. Adams, *Phys. Rev. Lett.* **36**, 1460 (1976).
- ¹⁸S. Takagi, *J. Phys. C* **8**, 1507 (1975).
- ¹⁹A. L. Fetter, *J. Low Temp. Phys.* **23**, 245 (1976).